Food and Chemical Toxicology 168 (2022) 113361

Contents lists available at ScienceDirect

Food and Chemical Toxicology

journal homepage: www.elsevier.com/locate/foodchemtox

Enniatins A1 and B1 alter calcium homeostasis of neuronal cells leading to apoptotic death

Nadia Pérez-Fuentes [a], Rebeca Alvariño [a,*], Amparo Alfonso [a,**], Jesús González-Jartín [a], Sandra Gegunde [a,b], Mercedes R. Vieytes [c], Luis M. Botana [a]

[a] Departamento de Farmacología, Facultad de Veterinaria, Universidad de Santiago de Compostela, Lugo, 27002, Spain
[b] Fundación Instituto de Investigación Sanitario Santiago de Compostela (FIDIS), Hospital Universitario Lucus Augusti, Lugo, 27002, Spain
[c] Departamento de Fisiología, Facultad de Veterinaria, Universidad de Santiago de Compostela, Lugo, 27002, Spain

ARTICLE INFO

Handling Editor: Dr. Jose Luis Domingo

Keywords:
Enniatins
Calcium fluxes
Apoptosis
Mitochondria
Combined toxicity

ABSTRACT

Enniatins (ENNs) A1 and B1 are non-regulated mycotoxins produced by *Fusarium* spp. that commonly occur in different types of food. These toxins are cytotoxic in several cell lines, but their mechanism of action is unclear. In this study, the cytotoxic effects of ENNs A1 and B1 in SH-SY5Y human neuroblastoma cells were analysed. Moreover, to better understand their mechanism of action, mitochondrial function, reactive oxygen species (ROS) levels and calcium fluxes were monitored. ENNs A1 and B1 reduced cell viability, presenting IC_{50} values of 2.0 and 2.7 μM, respectively. Both toxins induced caspase-dependent apoptosis, but only ENN A1 increased ROS production. Apoptotic cell death seems to be triggered by the increase in cytosolic calcium produced by both ENNs, since the toxins altered Ca^{2+} homeostasis by depleting intracellular reservoirs. Finally, binary combinations of ENN A1, ENN B1, ENN A and ENN B were tested. All mixtures resulted in an antagonistic effect, with the exception of ENN A and ENN B1 combination, which produced an additive effect. The results presented in this study provide the first evidence of ENNs A1 and B1 effects on calcium fluxes, providing new insights into the mechanism of action of these mycotoxins.

1. Introduction

Enniatins (ENNs) are cyclic hexadepsipeptidic mycotoxins mainly produced by *Fusarium* spp. This genus of fungus includes several species that affect crop and food contamination worldwide. Each *Fusarium* fungus can synthetize different types of mycotoxins including trichothecenes, fumonisins, zearalenone, beauvericin (BEA) and ENNs, among others (Sainz et al., 2018; Tonshin et al., 2010). The first three are included in the group of regulated mycotoxins by the European Commission (Commission Regulation (EC) No 1881/2006), so maximum limits of these toxins have been stablished in foodstuff. However, even though it was pointed out that ENNs are cytotoxic in the micromolar range (Prosperini et al., 2014), their concentrations in food are not regulated. This is due to the lack of information about the effects of these toxins, so they cannot be currently established as a health hazard (EFSA, 2014).

There are more than 29 ENNs analogues, being ENNs A, A1, B and B1 the most frequents ones. ENNs have similar chemical structures that consist in alternating a-hydroxy-D-isovaleric and N-methylamino acid moieties. ENN A1 is formed by a N-methyl-L valine moiety, two residues of N-methyl-L-isoleucine and three parts of a-hydroxy-D-isovaleric acid, whilst ENN B1 contains one moiety of N-methyl-L-isoleucine, two of N-methyl-L-valine and three of a-hydroxy-D-isovaleric acid (Wätjen et al., 2009) (Fig. 1). The non-regulated mycotoxin BEA is also a cyclohexadepsipeptide with three N-methyl-L-phenylalanine residues alternated with 2-hydroxy-D-isovaleric acid moieties (Bertero et al., 2020).

Due to their structural similarities, biological activities of ENNs and BEA have been traditionally related (Bertero et al., 2020). In 1973, it was proposed that ENN B formed complexes in biological membranes, allowing the passage of ions. Since then, ENNs and BEA cytotoxicity has been associated with their ionophoric properties (Ivanov et al., 1973; Kamyar et al., 2004). However, data about their ionophoric behaviour are scarce and most reports are focused on ENN B and BEA activities (Bertero et al., 2020; Tonshin et al., 2010). BEA induces apoptosis in

* Corresponding author.
** Corresponding author.
E-mail addresses: rebeca.alvarino@usc.es (R. Alvariño), amparo.alfonso@usc.es (A. Alfonso).

https://doi.org/10.1016/j.fct.2022.113361
Received 18 April 2022; Received in revised form 26 July 2022; Accepted 6 August 2022
Available online 12 August 2022

several cell lines (Jow et al., 2004; Lu et al., 2016; Pérez-Fuentes et al., 2021) and its cytotoxicity could be related with calcium homeostasis disruption, as the addition of a calcium chelator prevented BEA-induced cell death in human leukaemia cells (Jow et al., 2004). With respect to ENNs, it has been suggested that the mixture of the four ENNs has selective ionophoric properties for K^+ (Tonshin et al., 2010). Additionally, ENN B1 was recently reported to permeabilize the lysosomal membrane (Oliveira et al., 2020).

On the other hand, ENNs A, A1, B and B1 cytotoxicity could be related with mitochondrial impairment. These mycotoxins affect oxidative phosphorylation and mitochondrial volume regulation and cause apoptotic death through the production of reactive oxygen species (ROS) (Huang et al., 2019; Prosperini et al., 2013; Tonshin et al., 2010). Neuronal cells are very sensible to mitochondrial dysfunction and ion dysregulation due to their great dependence on oxygen consumption (Yin et al., 2014). In fact, ENNs A and B produced mitochondrial-mediated cytotoxicity in neuronal cells, and the analysis of natural contaminated samples containing the four ENNs revealed greater effects on neuronal viability than expected (Pérez-Fuentes et al., 2021), suggesting that their co-occurrence could suppose a health risk. However, neither the single nor the combined effects of ENNs A1 and B1 have been tested in neuronal cells so far.

Due to the previous results that point to an involvement of ion imbalance and mitochondrial dysfunction in the mechanism of action of ENNs, as well as their ability to cross the blood brain barrier (BBB) (Alonso-Garrido et al., 2021), ENNs A1 and B1 are expected to affect neuronal function and viability. Moreover, the increasing prevalence of ENNs contamination in Europe (González-Jartín et al., 2021; Prusova et al., 2022; Reinholds et al., 2021), as well as their potential bioaccumulation (Rodríguez-Carrasco et al., 2020) makes these toxins an inherent health hazard. Currently, data about their toxicity and bioactivity are still scarce and the need to elucidate their mechanism of action is increasingly evident. The present study examines the effects of ENN A1 and ENN B1 on cell viability, mitochondrial function, and calcium homeostasis in the human neuroblastoma cell line SH-SY5Y. In addition, binary combinations between these mycotoxins and ENNs A and B were tested to determine the potential consequences of their co-occurrence.

2. Materials and methods

2.1. Chemicals and solutions

CyQUANT™ lactate dehydrogenase (LDH) Cytotoxicity Assay Kit, tetramethyl rhodamine methyl ester (TMRM), 5-(and-6-)-carboxy-2′,7′-dichlorodihydrofluerescein diacetate (carboxy-H_2DCFDA), Dulbecco's Modified Eagle Medium: F-12 nutrient Mix (DMEM/F-12), glutamax, trypsin/EDTA (0.05%) and penicillin-streptomycin (10,000 U/mL) were purchased from Thermo Fisher Scientific (Madrid, Spain). ENN B1 (purity >99%) was bought in Vitro S.A. (Sevilla, Spain). Thapsigargin (Tg) was obtained from ENZO Life Sciences (Lausen, Swiss). ENN A, ENN A1 and ENN B (purity >95%), Annexin V-FITC Apoptosis Detection Kit, 3-(4,5-dimethyl thiazol-2-yl)-2,5-diphenyl tetrazolium bromide (MTT), Z-VAD-FMK, staurosporine (STS), saponin (SAP), and another chemical reagent grade were purchased from Merck (Madrid, Spain). ENNs standards were diluted in DMSO, and serial dilutions were prepared in culture medium. DMSO concentration was kept under 0.05% in all experiments.

The composition of Locke's buffer was (mM): NaCl 154.0, HEPES 10.0, KCl 5.6, glucose 5.0, $NaHCO_3$ 3.6, $CaCl_2$ 1.3 and $MgCl_2$ 1.0. The composition of Umbreit solution was (mM): NaCl 119.0, $NaHCO_3$ 22.85, KCl 5.94, $Mg(SO)_4$ 1.2, NaH_2PO_4 1.2, Glucose 0.1% and $CaCl_2$ 1.0. The pH was adjusted between 7.2 and 7.4 in all the assays. Phosphate buffered saline (PBS) was composed of (mM): NaCl 137.0, Na_2HPO_4 8.2, KH_2PO_4 1.5 and KCl 3.2 (pH 7.4).

2.2. Cell culture and treatment

SH-SY5Y human neuroblastoma cells were obtained from American Type Culture Collection (ATCC), number CRL2266. Cells were maintained in DMEM/F-12 medium supplemented with 10% foetal bovine serum (FBS), 10,000 U/mL penicillin-streptomycin and 1% glutamax at 37 °C in a humidified atmosphere of 95% air and 5% CO_2. Cells were dissociated once a week using 0.05% trypsin/EDTA.

2.3. Cell viability assay

The effects of ENNs on SH-SY5Y cells viability was analysed using MTT assay as previously described (Kumar et al., 2018; Pérez-Fuentes et al., 2021). Cells were seeded at 5×10^4 cells per well in 96-well plates and allowed to grow for 24 h. Then, cells were treated with ENN A1 and B1 at concentrations ranging from 0.1 to 15 μM for 6 and 24 h. After treatment, cells were washed three times with 200 μL/well of Locke's solution. Then, 200 μL of MTT (500 μg/mL) were added to each well and the plate was incubated in an orbital shaker for 1 h at 300 rpm and 37 °C. Afterward, MTT was removed, and cells were lysed by adding 5% sodium dodecyl sulphate. The absorbance originated was read at 595 nm in a spectrophotometer plate reader. SAP from *Quillaja bark* (1 mg/mL) was used as cell death control and its absorbance was subtracted from the other data.

To determine if ENN A1 and ENN B1 produced caspase-mediated apoptosis, SH-SY5Y cells were pre-treated with the caspase inhibitor Z-VAD-FMK at 40 μM for 24 h. Then, ENN A1 and ENN B1 at half

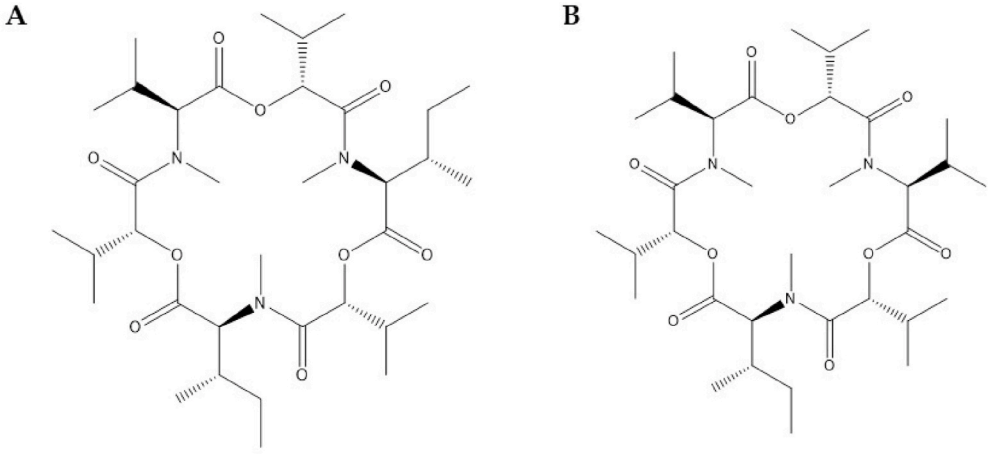

Fig. 1. Chemical structure of enniatins A1 (A) and B1 (B).

inhibitory concentrations (IC_{50}) were added for 24 h and MTT assay was performed.

For combination assays, ENNs (A, A1, B and B1) were mixed at 1:1 ratio, mimicking the proportion found in contaminated samples from NW Iberian Peninsula (González-Jartín et al., 2021). For this experiment, cells were seeded in 384-well plates at 2.5×10^4 cells per well. Neuroblastoma cells were treated with binary combinations for 24 h and MTT assay was carried out as described above.

All experiments were performed three times by triplicate.

2.4. Cytotoxicity assay

To analyse the effects of individual and mixed mycotoxins on cell cytotoxicity, CyQUANT™ LDH Cytotoxicity Assay Kit test was used, following manufacturer's instructions (Pérez-Fuentes et al., 2021). SAP from *Quillaja bark* at 1 mg/mL was used as cell death control. Cells were treated with ENNs A1 and B1 at concentrations from 0.1 to 15 μM for 6 and 24 h, whilst binary combinations were performed for 24 h, as described above. LDH release was evaluated after transferring 50 μL of cell medium to a 96-well flat-bottom. Absorbance was read at 490 and 680 nm in a plate reader. Finally, the background signal (680 nm absorbance value) was subtracted from the 490 nm absorbance value to determine LDH release to the medium. Experiments were performed three independent times by triplicate.

2.5. Mitochondrial membrane potential measurement

TMRM dye was used to analyse mitochondrial membrane potential ($\Delta\Psi_m$) (Pérez-Fuentes et al., 2021). Human neuroblastoma cells were seeded in 96-well plates at 5×10^4 cells per well and allowed to attach for 24 h. Then, cells were treated with ENN A1 and ENN B1 for 6 and 24 h. After this time, the plate was washed twice with Locke's solution, TMRM 20 μM was added, and the plate was incubated 30 min at 300 rpm and 37 °C. Then, the dye was removed, cells were dissolved in H_2O and DMSO (1:1) and fluorescence was read at 535 nm excitation and 590 nm emission in a plate reader. Rotenone (Rot) at 1 μM was used as positive control. Assays were performed by triplicate three independent times.

2.6. Measurement of intracellular reactive oxygen species levels

The fluorescent dye carboxy-H_2DCFDA was used to measure the levels of ROS produced by neuroblastoma cells as described before (Alvariño et al., 2021). After treatment with ENN A1 and ENN B1 for 6 and 24 h, cells were washed twice with serum-free medium. At that point, 20 μM carboxy-H_2DCFDA diluted in serum-free medium was added, and cells were incubated in an orbital shaker for 1 h at 300 rpm and 37 °C. Then, PBS was added to every well and the plate was incubated for 30 min at 300 rpm and 37 °C. Finally, fluorescence was read at 495 nm excitation and 527 nm emission in a plate reader. H_2O_2 150 μM was used as positive control. Experiments were performed in triplicate three times.

2.7. Cell death type analysis

To determine the cell death type produced by the toxins, Annexin V-FITC Apoptosis Detection Kit was used, following manufacturer's instructions (Pérez-Fuentes et al., 2021). For this assay, cells were seeded in 12-well plates at 5×10^5 cells per well. After 24 h, cells were treated with ENN A1 and ENN B1 and incubated another 24 h. STS at 0.1 μM was used as positive control. Then, cells were washed with PBS, resuspended in Annexin-binding buffer containing Annexin V-FITC and Propidium Iodide (PI) and incubated for 15 min at room temperature. Cells were resuspended in commercial PBS (pH 7.2) (Thermo Fisher Scientific), filtered, and kept on ice. Next, fluorescence was analysed by flow cytometry using the ImageStreamMKII instrument (Amnis Corporation, Luminex Corp, Austin, TX, USA). IDEAS Application 6.0 software was used to determine the fluorescence of 10,000 events (Amnis Corporation, Luminex Corp).

2.8. Measurement of cytosolic free calcium

Cells were seeded in 18-mm glass coverslips at 5×10^5 cells per well and incubated for 24 h. For calcium measurement, cells were washed twice with Umbreit solution, enriched with 0,1% BSA. SH-SY5Y cells were loaded with the fluorescent dye FURA-2 AM (0.5 μM) for 6.5 min at 300 rpm and 37 °C. Then, cells were washed twice with Umbreit solution and coverslips were placed in a thermostatic chamber (Life Sciences Resources, UK) (Sánchez et al., 2015). Cells were viewed in an inverted microscope Nikon Diphot 200, equipped with epifluorescence optics (Nikon 40x, immersion UV-fluor objective). Mycotoxin dilution was made in Umbreit solution without calcium, and compounds were directly added to the incubation chamber. Cytosolic calcium levels as FURA-2 ratio were obtained from the images collected by fluorescence equipment, consisting in an ultra-high-speed wavelength switcher (Lambda-DG4) for excitation and an optical filter changer Lambda 10–2 for emission (Sutter Instruments Co., USA). The light source was a xenon arc bulb and wavelengths used were selected with the filters. Cells were excited at 340 and 380 nm, with emission at 505 nm.

2.9. Statistical analysis

Data are presented as mean ± SEM of three independent experiments. Differences were evaluated by One-way ANOVA followed by Dunnett's or Tukey's multiple comparison tests. Statistical significance was established at $^*p < 0.05$, $^{**}p < 0.01$, and $^{***}p < 0.001$. IC_{50} and half maximal effective concentration (EC_{50}) values were calculated with GraphPad Prism 8 software by fitting the data with a log(inhibitor) *vs* response or a log(agonist) *vs* response models, respectively.

The combination index was calculated with Chou & Talalay equation (Chou and Talalay, 1983):

$$COMBINATION\ INDEX = \frac{D1}{(DX)1} + \frac{D2}{(DX)2}$$

where (DX)1 and (DX)2 are IC_{50} values of each mycotoxin alone, and D1 and D2 are IC_{50} values of each mycotoxin in combination. If the results of the equation are <1, =1 and >1, Chou & Talalay method considers synergism, additivity, or antagonism, respectively.

3. Results

3.1. Evaluation of ENN A1 and B1 effects on viability, mitochondrial function, and calcium homeostasis of SH-SY5Y cells

At first, effects of ENNs A1 and B1 on cell survival were evaluated with two assays. MTT dye was used to analyse the effects of ENNs in cell viability, whilst cytotoxicity was determined by LDH assay. Dose-response treatments were performed (0.1–15 μM) for 6 and 24 h and the experiments were carried out. Regarding MTT test, which determines cell viability based on cell metabolism, ENN A1 treatment for 6 h reduced cell viability between 36.2 and 99.7% at concentrations over 2.5 μM. After 24 h, cell viability decrease was greater, with a diminution of 88.3 ± 6.0% ($p < 0.001$) at 2.5 μM (Fig. 2 A). In the case of ENN B1, this toxin significantly decreased SH-SY5Y cell viability at 2.5, 5, 10 and 15 μM after 6 h of treatment. At longer incubation times (24 h), cell viability was reduced between 44.6 and 100% at doses higher than 2.5 μM (Fig. 2 B). With the data obtained in MTT assays, IC_{50} values for each toxin were calculated by fitting the data with a log(inhibitor) *vs* response model (Fig. S1 A-B). At 6 h of incubation, ENN A1 and ENN B1 showed similar IC_{50} values, 3.4 μM (CI: 2.8–4.4 μM) and 3.0 μM (CI: 2.4–3.6 μM), respectively. After 24 h incubation, IC_{50} values were lower, being ENN A1 (2.0 μM, CI: 1.2–3.3 μM) a little more damaging than ENN B1 (2.7

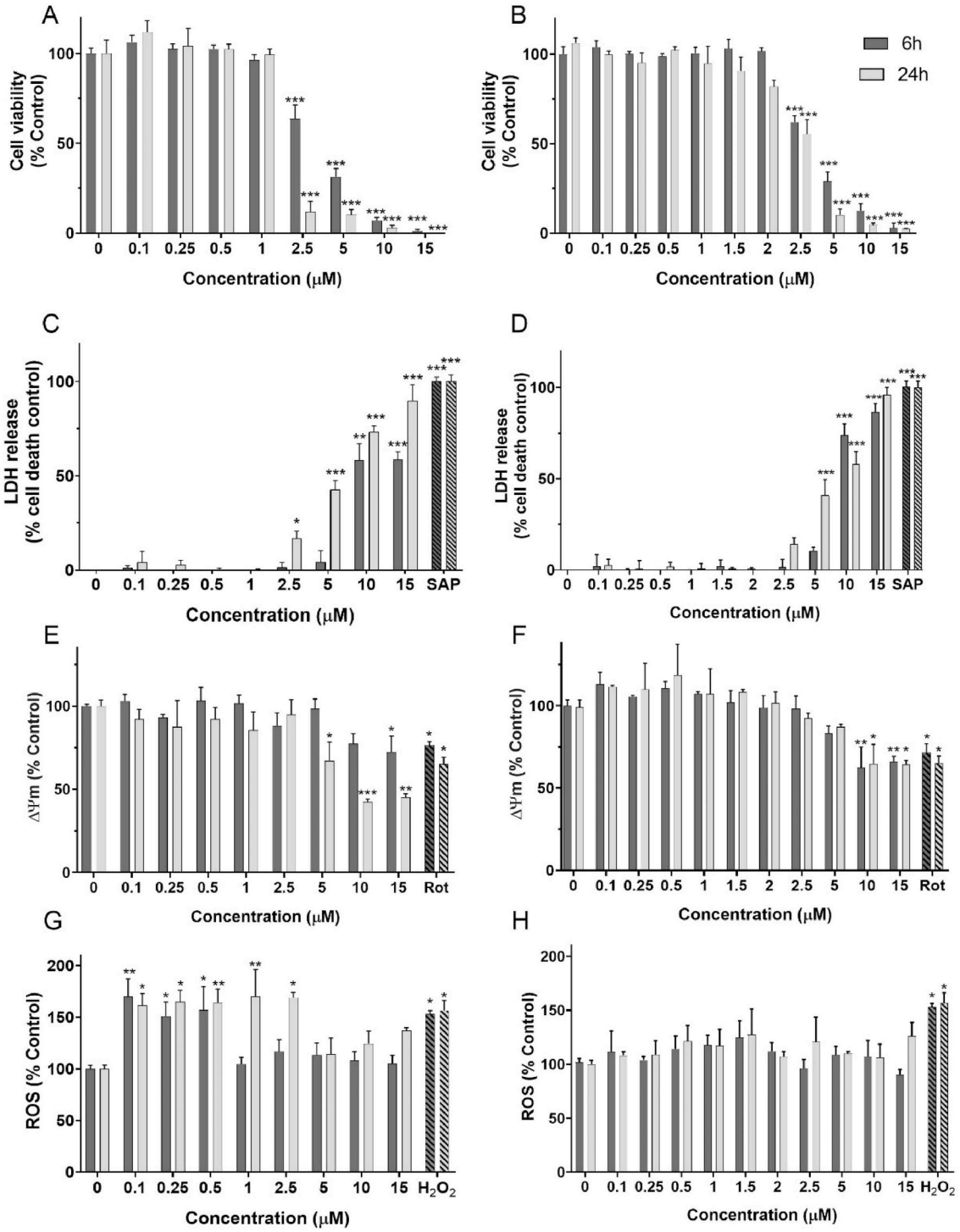

Fig. 2. Effects of ENNs A1 and B1 on viability and mitochondrial function of SH-SY5Y cells. Cells were treated with ENNs for 6 and 24 h. (A) Effect of ENN A1 and (B) ENN B1 on cell viability, assessed by MTT test. (C) Cytotoxicity of ENN A1 and (D) ENN B1, determined by LDH assay. Saponin (SAP) at 1 mg/mL was used as cell death control. (E) Mitochondrial membrane potential ($\Delta\Psi_m$) after treatment with ENN A1 and (F) ENN B1, measured using TMRM dye. Rot at 1 μM was used as positive control. (G) ROS levels after treatment with ENN A1 and (H) ENN B1, assessed by using carboxy-H_2DCFDA dye. 150 μM H_2O_2 was used as positive control for ROS production. Data are mean ± SEM of three independent replicates. Statistical differences determined by One-way ANOVA and Dunnett's multiple comparison test. *$p \leq 0.05$, **$p \leq 0.01$ and ***$p \leq 0.001$, significantly different from the control.

μM, CI: 2.4–3.1 μM).

As explained before, cytotoxicity was assessed with LDH assay, which provides information about cell membrane damage, and therefore has lower sensitivity than MTT assay. Results agreed with those obtained with MTT test, observing LDH release at the highest concentrations used (Fig. 2C–D). ENN A1 increased LDH liberation about 58% at concentrations above 10 μM after 6 h of treatment. At 24 h, the augmentation in LDH levels ranged between 20.2 and 89.9% at concentrations higher than 2.5 μM (Fig. 2 C). Finally, ENN B1 showed a significant increase in LDH release at doses above 10 μM after 6 h incubation, reaching levels of 88.7 ± 4.4% ($p < 0.001$) at 15 μM. After 24 h of exposure, ENN B1 induced a rise in LDH levels among 41.0–98.0%

(Fig. 2 D). From these data, EC_{50} values for each toxin were calculated by fitting the data with a log(agonist) *vs* response model (Fig. S1 C-D). ENN B1 presented an EC_{50} of 7.4 μM (CI: 6.4–8.3 μM) after 6 h of incubation. At longer treatments, EC_{50} of both toxins were similar, 6.2 μM (CI: 4.6–13.6 μM) and 6.7 μM (CI: 5.8–7.8 μM) for ENN A1 and ENN B1, respectively.

In view of the results obtained with MTT and LDH assays, the effects of ENNs on mitochondrial function were evaluated. Cells were treated with ENNs A1 and B1 for 6 and 24 h at the same concentrations used before. Then, $\Delta\Psi_m$ and ROS production were analysed. To study how compounds affected $\Delta\Psi_m$, the fluorescent dye TMRM was used, and the assay was validated with the inhibitor of the electronic transport chain Rot at 1 μM. Since $\Delta\Psi_m$ is maintained by oxidative phosphorylation, it is an indicator of mitochondrial function. As Fig. 2 E-F shows, both ENNs depolarized the mitochondrial membrane at the highest dosed used after 6 and 24 h of treatment. ENN A1 produced significant differences compared to control cells at 15 μM (72.4 ± 9.7%, $p < 0.05$) after 6 h of incubation. At 24 h, this toxin affected mitochondrial function at concentrations above 5 μM, reducing $\Delta\Psi_m$ by 45.2 ± 2.1% ($p < 0.01$) at 15 μM (Fig. 2 E). ENN B1 produced a lower effect, depolarizing mitochondrial membrane between 35.0 and 37.5% of control cells at 10 and 15 μM at both times of incubation (Fig. 2 F). These levels were similar to those observed after addition of the positive control Rot, which affected mitochondrial membrane at both times between 28.4 and 34.8% of control cells.

As mitochondria are the main producers of ROS in cells, effect of ENNs on release of these damaging molecules was analysed. ENN A1 induced an increase in ROS production at several concentrations (Fig. 2 G). At 6 h, this compound elevated ROS generation at doses between 0.1 and 0.5 μM about a 50% of control cells. Furthermore, treatment with ENN A1 for 24 h also augmented ROS at the lower doses, reaching an increase of 169.0 ± 4.9% ($p < 0.05$) at 2.5 μM. Conversely, ENN B1 did not produced ROS release at any concentration (Fig. 2 H). The assay was validated with H_2O_2 at 150 μM, treatment that increased ROS levels up to 153.0 ± 3.2 μM ($p < 0.05$) and 156.7 ± 9.5 μM ($p < 0.05$) at 6 and 24 h, respectively.

Since ENNs A1 and B1 affected cell viability, the type of death produced by these mycotoxins was evaluated. Cells were treated with ENNs for 24 h at IC_{50} values calculated with MTT test and the apoptosis inductor STS at 1 μM was used as positive control. Next, co-staining Annexin V-FITC and PI was carried out and fluorescence was analysed by flow cytometry (Fig. 3A–B). Percentages of early and late apoptotic cells (Annexin V-FITC positive and PI positive or negative) and necrotic cells (Annexin V-FITC negative and PI positive) were calculated. ENNs A1 and B1 produced a significant increase in apoptotic cells of 39.3 ± 5.1% ($p < 0.01$) and 36.3 ± 0.5% ($p < 0.05$), respectively, without any change in the percentage of necrotic cells, compared to control. As expected, the apoptotic inducer STS increased cells in apoptosis (45.2 ± 5.7%, $p < 0.01$).

To further confirm that ENNs were producing caspase-dependent apoptosis, the caspase inhibitor Z-VAD-FMK was used (Fig. 3 C). Cells were pre-treated with Z-VAD-FMK for 24 h, followed by exposure to ENNs A1 and B1, and cell viability was assessed. As observed in control cells, pre-treatment with the inhibitor did not affect cell viability. Regarding ENN A1, a decrease in cell viability of 16.8 ± 3.3% ($p < 0.05$) was observed when cells were pre-treated with Z-VAD-FMK. This reduction was significantly smaller ($p < 0.05$) than the diminution produced by the toxin alone (37.6 ± 0.9%, $p < 0.001$). Similar results were obtained with ENN B1, which presented a reduction of 18.5 ± 6.0% ($p < 0.05$) in cells pre-treated with the caspase inhibitor and a

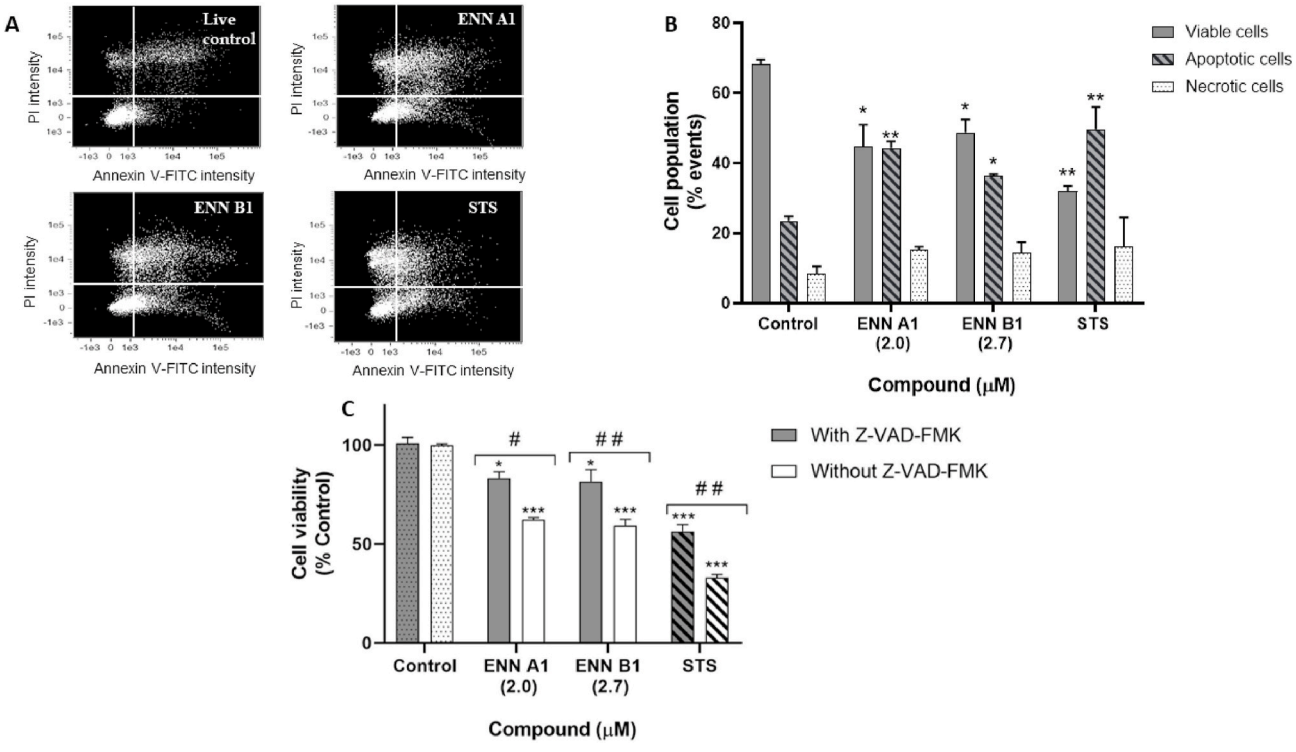

Fig. 3. Analysis of cell death type induced by ENNs A1 and B1 in SH-SY5Y cells. (A) Representative scatter plot of flow cytometry analysis. (B) Bar graph of the results obtained by flow cytometry. Cells were treated with mycotoxins at IC_{50} values for 24 h, co-stained with Annexin V-FITC and PI, and the fluorescence of 10000 cells was monitored. Percentages of viable cells (Annexin V-FITC -/PI -), apoptotic cells including early apoptosis (Annexin V-FITC + /PI –) and late apoptosis (Annexin V-FITC + /PI +), and necrotic cells (Annexin V-FITC –/PI+) were calculated. Data are mean ± SEM of three independent experiments, compared to control cells by One-way ANOVA followed by Dunnett tests (*$p \leq 0.05$ and **$p \leq 0.01$). (C) Evaluation of caspases involvement in ENNs-induced apoptosis. Cells were pre-treated with 40 μM Z-VAD-FMK for 24 h, followed by addition of ENNs at IC_{50} values, and cell viability was analysed. STS was used as positive control in these assays. Mean ± SEM of three independent experiments, expressed as percentage of control cells. Statistical significance determined by One-way ANOVA and Tukey's test (*$p \leq 0.05$ and ***$p \leq 0.001$, compared to control cells), (#$p \leq 0.05$ and ##$p \leq 0.01$, compared to their corresponding control).

decrease of 40.6 ± 3.1% ($p < 0.001$) when ENN B1 was added alone. These results were significantly different ($p < 0.01$), confirming that caspases are involved in the apoptosis generated by ENN B1. The assay was validated with STS (1 μM), which also presented a significant difference ($p < 0.01$) between pre-treated and non-pre-treated cells.

Finally, the effects of ENNs A1 and B1 on cytosolic Ca^{2+} were assessed. Tg at 2 μM was used as positive control. This compound inhibits irreversibly the Ca^{2+}-ATPase from the endoplasmic reticulum (ER), inducing Ca^{2+} pools depletion to cytosol and subsequently activating the entry of this ion through membrane store-operated channels (SOC). Tg effects were well documented and previously described in SH-SY5Y cells (Sánchez et al., 2015).

A dose-response assay was first performed with each mycotoxin. ENN A1 was tested at 0.5, 1 and 2 μM, while ENN B1 was used at 1, 2 and 5 μM. As Fig. 4 A-B shows, both ENNs act in a dose-dependent manner. However, each ENN seems to act differently. ENN A1 produced an acute Ca^{2+} depletion from intracellular compartments, and significantly increased Ca^{2+} uptake when this ion was added to the bath solution. At the highest dose employed (2 μM), Ca^{2+} uptake after adding the ion to the bath solution reached similar levels than Tg (Fig. 4 A). In the case of ENN B1, Ca^{2+} depletion from intracellular pools was smoother than the originated by ENN A1. Moreover, this toxin also induces Ca^{2+} entry when the ion was added to the bath solution, but it was smaller than the effect produced by ENN A1 (Fig. 4 B).

As ENN A1 exhibited a similar profile than the produced by Tg, it was checked if this mycotoxin was affecting the same reservoirs depleted by Tg. With this objective, ENN A1 and Tg and *vice versa*, were consecutively added to neuroblastoma cells. Fig. 4 C shows that pre-incubation with 2 μM ENN A1 did not inhibit Tg-induced Ca^{2+} depletion from ER. Moreover, pre-addition of ENN A1 increased calcium uptake when this ion was incorporated to the bath solution in comparison to cells treated with Tg alone. When Tg was added in first place, the effects of ENN A1 were reduced compared to those produced by the mycotoxin alone. When Ca^{2+} was added to the bath solution, the uptake of this ion was similar than the produced by ENN A1 and Tg alone (Fig. 4 D). However, this influx did not result in Ca^{2+} levels as high as those produced by adding first ENN A1, rather than Tg, to the cells.

3.2. Evaluation of ENNs binary combinations toxicity

In order to investigate interactions between ENNs, they were binary combined, and their toxic effects were determined. Concentration ratio (1:1) was selected based on the most frequent proportions found in samples from NW Iberian Peninsula (González-Jartín et al., 2021). As ENNs A1 and B1 usually appear in combination with ENN A and B, their combined effects were also tested. In this context, ENNs were combined as follows: ENN A1 + ENN A, ENN B1+ ENN A, ENN A1 + ENN B, ENN B1 + ENN B and ENN A1 + ENN B1. Concentration range (0.1–10 μM) and incubation time (24 h) were chosen based on the results obtained in the previous experiments.

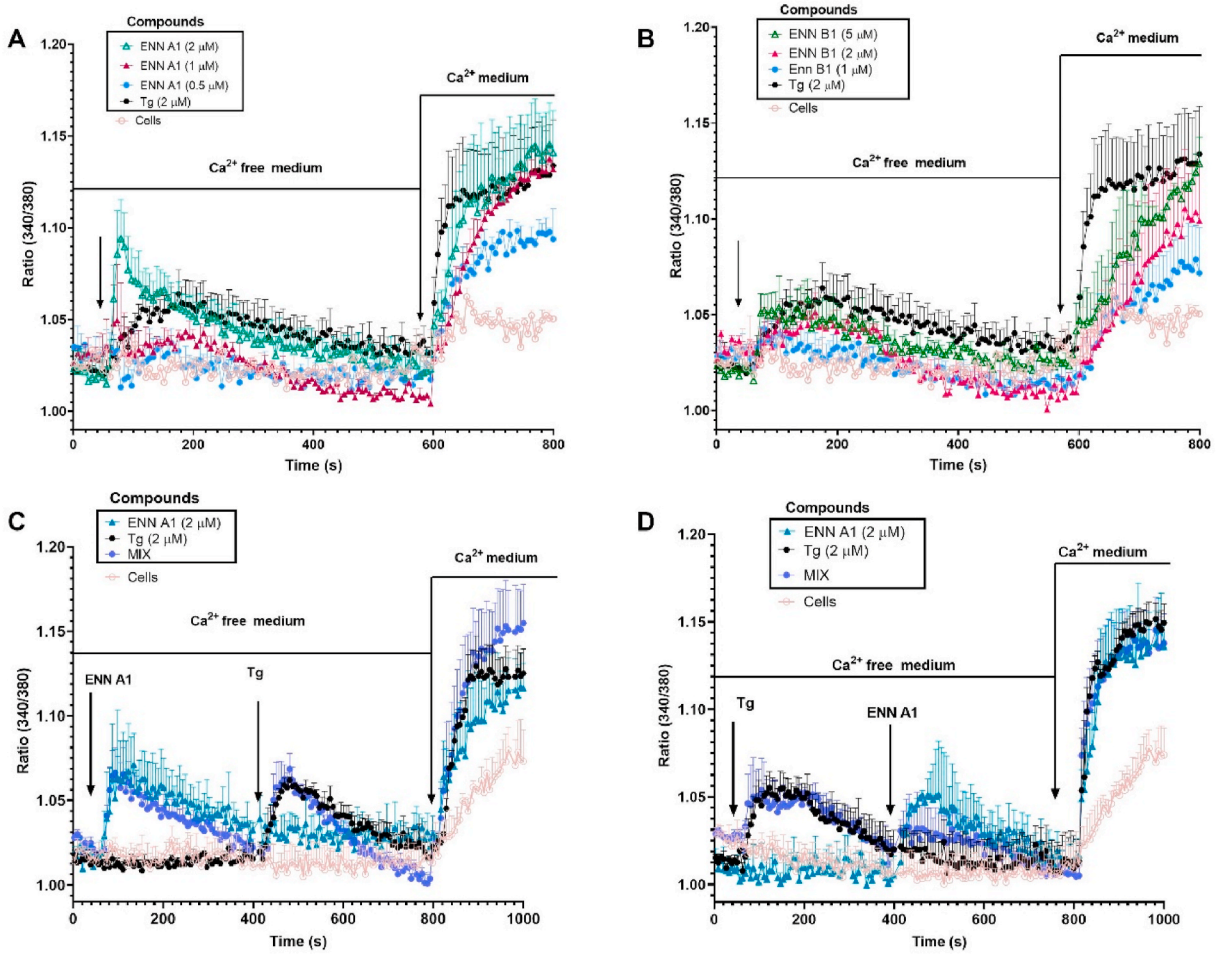

Fig. 4. Effects of ENNs A1 and B1 on cytosolic Ca^{2+} profile of SH-SY5Y cells. (A) ENN A1 dose-response assay. (B) ENN B1 dose-response assay. Tg at 2 μM was used as positive control. The first arrow indicates the addition of compounds. The second arrow shows the addition of 1 mM of Ca^{2+} to the bath solution. (C) Cytosolic Ca^{2+} profile of cells pre-incubated with 2 μM ENN A1 (first arrow) followed by addition of Tg at 2 μM (second arrow). Third arrow indicates the addition of 1 mM of Ca^{2+} to the bath medium. (D) Cytosolic Ca^{2+} profile of cells pre-treated with Tg at 2 μM (first arrow) followed by 2 μM ENN A1 (second arrow). Third arrow indicates the addition of 1 mM of Ca^{2+} to the bath medium. Mean ± SEM of three independent experiments performed by duplicate.

Initially, the effect of binary combinations on cell viability was determined with MTT test. The results obtained with ENN A1 + ENN A were similar to those observed after treatment with ENN A1 alone. This mixture caused a significant decrease on cell viability at concentrations above 1.5 μM, reaching a reduction of 96.6 ± 1.2% ($p < 0.001$) at 10 μM (Fig. 5 A). In the case of ENN B1 + ENN A, the results were quite similar to the previous mixture, inducing almost a complete decrease at the highest concentration used (Fig. 5 B). Regarding ENN A1 + ENN B, levels of cell viability ranged between 45.7 and 10.2% at concentrations higher than 1.5 μM (Fig. 5 C). On the other hand, the cell damage caused by ENN B1 + ENN B was less pronounced than in the previous mixtures, reducing cell viability by 86.2 ± 1.2% (Fig. 5 D) at 10 μM. Finally, ENN A1 + ENN B1 also injured cells at concentrations above 1 μM (Fig. 5 E).

With the results obtained in MTT assay, IC_{50} values for each combination were determined (Table 1, Fig. S2). With single and combined IC_{50} data, and following Chou & Talalay method, combination index was calculated (Chou and Talalay, 1983). IC_{50} values from ENN A and ENN B in SH-SY5Y cells after 24 h of incubation had been previously determined (2.3 and 0.4 μM, respectively) (Pérez-Fuentes et al., 2021). Chou & Talalay method establishes that if combination index is higher than 1, the toxins mixture produces antagonism, if it is equal to 1, it is an additive effect, and if it is lower than 1, it will be due to a synergistic effect. Except for ENN B1 + ENN A mixture, all combination indexes were higher than 1, indicating an antagonistic effect between the toxins. In the case of ENN B1 + ENN A, combination index value was 1.0, denoting an additive effect.

Finally, cytotoxicity of binary mixtures was assessed with LDH assay (Fig. 6). All the combinations originated an increase in LDH release at concentrations higher than 2.5 μM, but only ENN A1 + ENN A, ENN B1 + ENN A and ENN A1 + ENN B1 reached levels similar to the cell death control (94.0 ± 10.1%, 78.4 ± 9.8% and 91.1 ± 11.9%, $p < 0.001$, respectively). The other combinations produced a maximum augmentation of LDH levels in cell supernatant about 41%.

With the results obtained in LDH assay, EC_{50} values were calculated (Fig. S3). Except for ENN B combinations, whose EC_{50} value could not be calculated, the other mixtures showed lower or similar values to those of ENNs A1 and B1 alone. EC_{50} of ENN A1 + ENN A mixture was 4.4 μM (CI: 3.9–4.9 μM). ENN B1 + ENN A combination presented an EC_{50} of 6.8 μM (CI: 6.0–7.8 μM), whilst ENN A1 + ENN B1 showed a value of 4.3 μM (CI: 3.6–5.2 μM).

Table 1
IC_{50} and combination index of enniatins mixtures. ENN A: enniatin A, ENN A1: enniatin A1, ENN B: enniatin B and ENN B1: enniatin B1, CI: 95% confidence interval.

Binary combination (1:1)	IC_{50} (μM)	Combination index
ENN A1 + ENN A	1.7 (CI: 1.5–1.9) R^2: 0.94	1.7
ENN B1 + ENN A	1.3 (CI: 0.76–2.3) R^2: 0.89	1.0
ENN A1 + ENN B	1.4 (CI: 1.2–1.6) R^2: 0.92	4.2
ENN B1 + ENN B	1.4 (CI: 1.1–1.8) R^2: 0.88	4.1
ENN A1 + ENN B1	1.5 (CI: 1.2–1.8) R^2: 0.94	1.3

4. Discussion

ENNs are non-regulated mycotoxins that commonly occur in grain and another foodstuff at concentrations in the micromolar range. In the last decades, there have been few studies about ENNs toxicity and their mechanism of action is still unclear (Bertero et al., 2020). Most works analysed the cytotoxicity produced by ENNs in intestinal or liver cell lines because the main route of exposure is through ingestion (Meca et al., 2010, 2011). In this study, two of the most frequent ENNs found in cereals of Europe, ENN A1 and ENN B1, were chosen to determine how they affect SH-SY5Y human neuroblastoma cells (Gautier et al., 2020). Experiments were carried out in a neuronal cell line because it has been described that ENNs can cross the BBB due to their lipophilic nature (Alonso-Garrido et al., 2020). In these cells, ENN A1 and ENN B1 affected cell viability, presenting IC_{50} values in the micromolar range at both incubation times. These values were lower than those previously reported in intestinal or liver cells. SH-SY5Y cells were found to be 5–7 times more sensitive to ENNs A1 and B1, suggesting that they could be neurotoxic at concentrations found in contaminated samples. In fact, treatment with a mixture of ENNs and BEA in an *in vitro* model of BBB produced a downregulation in the expression of the complex I of the electronic transport chain. This impairment has been related to

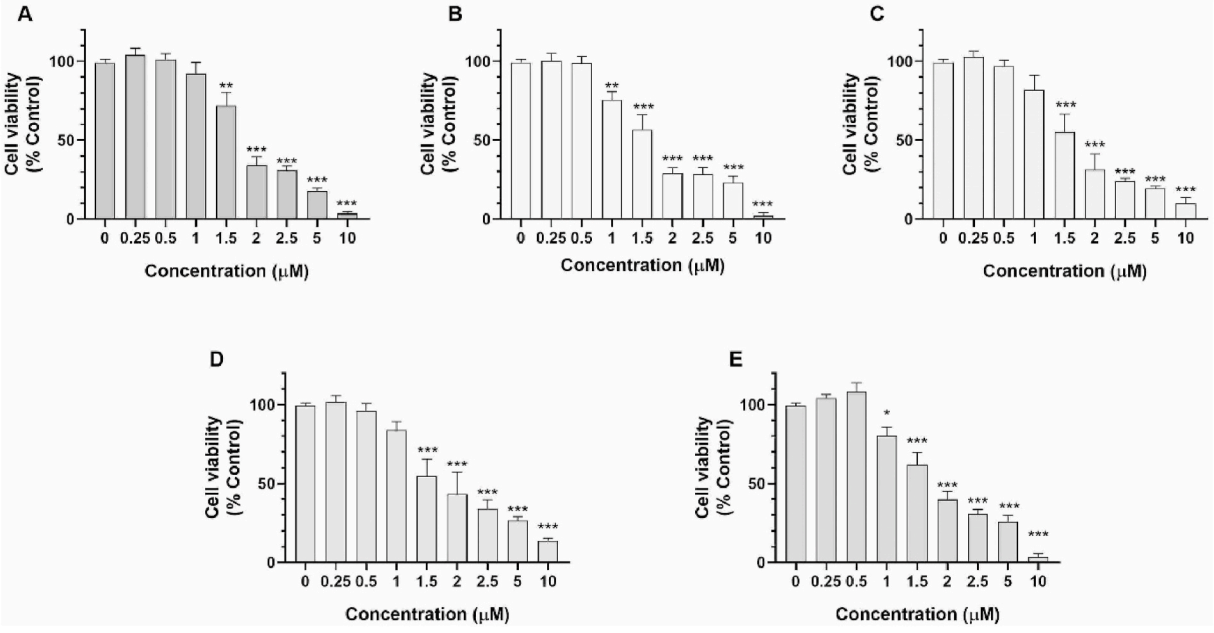

Fig. 5. Effects of ENNs binary combinations in cell viability of SH-SY5Y cells. Human neuroblastoma cells were treated with binary mixtures (1:1) of ENNs A1, B1, A, and B for 24 h and their effect on cell viability was assessed with MTT assay. (A) ENN A1 + ENN A, (B) ENN B1 + ENN A, (C) ENN A1 + ENN B, (D) ENN B1 + ENN B and (E) ENN A1 + ENN B1. Data are mean ± SEM of three independent replicates expressed as percentage of untreated control cells. Statistical differences determined by One-way ANOVA and Dunnett's multiple comparison tests. *$p \leq 0.05$, **$p \leq 0.01$ and ***$p \leq 0.001$, significantly different from the control.

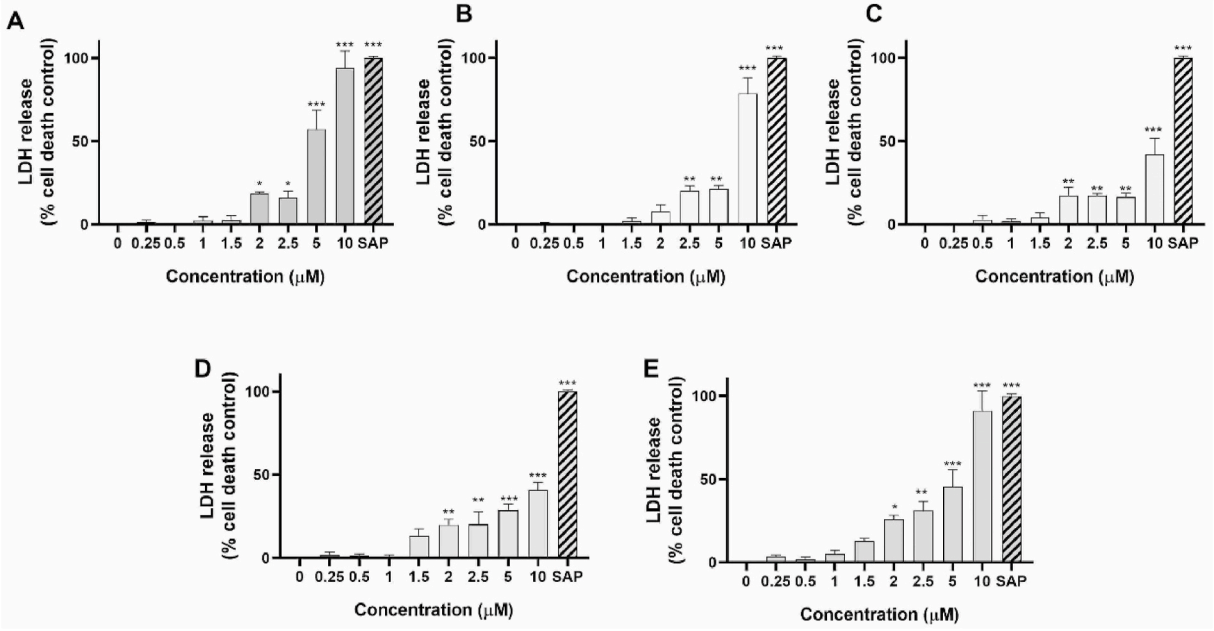

Fig. 6. Cytotoxic effects of ENNs binary combinations in human neuroblastoma cells. SH-SY5Y cells were treated with ENNs mixtures (1:1) for 24 h and cytotoxicity was determined by LDH assay. (A) ENN A1 + ENN A, (B) ENN B1 + ENN A, (C) ENN A1 + ENN B, (D) ENN B1 + ENN B and (E) ENN A1 + ENN B1. SAP (1 mg/mL) was used as cell death control. Data are mean ± SEM of three independent replicates expressed as percentage of cell death control. Statistical differences determined by One-way ANOVA and with Dunnett's multiple comparison test. *p ≤ 0.05, **p ≤ 0.01 and ***p ≤ 0.001, significantly different from untreated control cells.

neurodegenerative diseases, supporting the assumption that ENNs exert neurotoxic effects (Alonso-Garrido et al., 2021).

The results obtained in MTT and LDH assays coincide for both mycotoxins, since the reduction of cell viability matches with the increase in LDH release. Considering that MTT is mainly metabolised by mitochondria (Fotakis and Timbrell, 2006), cytotoxicity produced by ENNs in neuroblastoma cells could be related with mitochondria impairment, as it was seen in the BBB model mentioned above (Alonso-Garrido et al., 2021). For this reason, the effects of ENNs A1 and B1 on $\Delta\Psi_m$ and ROS production were assessed. Surprisingly, both ENNs only affected $\Delta\Psi_m$ at highest doses used, so this reduction seems to be associated to the decrease in cell survival produced by these mycotoxins at those concentrations. Their analogues ENN A and ENN B produced mitochondrial depolarization at doses between 0.1 and 10 μM under the same conditions, suggesting that the mechanism of action of ENNs A and B is more related to mitochondria (Pérez-Fuentes et al., 2021). On the other hand, when analysing ROS production, ENN A1 elevated ROS levels in a wide range of concentrations while ENN B1 did not affect the release of these damaging molecules. In Caco-2 cells, ENN B1 was shown to elevate ROS generation, so intestinal cells seem to be more prone to originate ROS than neuronal cells after treatment with this toxin (Prosperini et al., 2013). Since ENN A1 increased ROS release at low doses without affecting $\Delta\Psi_m$, it seems that the toxin acts through a different pathway such as NADPH oxidase activation (Tarafdar and Pula, 2018). In any case, the lack of effect of ENN B1 on ROS release points to a different mechanism of action of each ENN.

Despite these differences, both ENNs A1 and B1 induced apoptotic death in human neuroblastoma cells, as did their analogues ENNs A and B (Pérez-Fuentes et al., 2021). Moreover, the results obtained with the caspase inhibitor suggest that ENNs A1 and B1 induce caspase-dependent apoptosis. The involvement of these enzymes in cytotoxicity of ENN A1, ENN B1 and ENN B had already been described in other cell types (Manyes et al., 2018; Wätjen et al., 2009). It is known that Ca^{2+} is involved in the activation of some caspases and that apoptosis could be associated with calcium signalling (Carreras-Sureda et al., 2018). Moreover, it has been suggested that ENNs have ionophoric properties and form membrane channels that permit the passage of ions (Kamyar et al., 2004). Therefore, the effects on calcium homeostasis of ENN A1 and B1, which had not been described before, were analysed. ENNs A1 and B1 produced Ca^{2+} depletion from intracellular reservoirs and increased Ca^{2+} uptake in a dose-dependent manner, but the way these toxins affected calcium homeostasis seems to be different. ENN A1 produced a depletion of Ca^{2+} from intracellular pools similar to the response observed when Tg, an inhibitor of the ER Ca^{2+}-ATPase, was added. Otherwise, ENN B1 generated a smaller ion depletion, suggesting that ENNs A1 and B1 altered ion homeostasis through different pathways. As the calcium profile of the ENN A1 resembled the response produced by Tg, it was determined if both compounds affected the same cell channels. The results obtained suggest that ENN A1 is affecting the ER and to other calcium reservoirs in a reversible way. When cells were treated with ENN A1 before Tg addition, the response of the latter was not altered, so the effects produced by the mycotoxin on ER seem to be reversible. Otherwise, when Tg, an irreversible inhibitor of ER Ca^{2+}-ATPase, was added before ENN A1, the effect of the toxin on intracellular pools depletion was smaller, but it was still a response, suggesting that it affects other cell compartments. As mitochondria are the second organelles with greater Ca^{2+} retention capacity, ENN A1 could be emptying this reservoir (Carreras-Sureda et al., 2018).

Therefore, the results point to a calcium-mediated apoptosis produced by ENN A1, in which ROS generation might be involved. Similar effects have been seen with the related mycotoxin BEA, whose effects on apoptosis were reversed by the addition of a calcium chelator (Chen et al., 2006). In the case of ENN B1, its cytotoxic effects on neuronal cells also occur through apoptosis. Calcium dysregulation seems to be involved in its mechanism of action, but mitochondrial dysfunction and oxidative stress are not implicated. With these data, it cannot be clearly confirmed if ENN A1 and ENN B1 are ionophores, but these toxins display different effects on calcium fluxes. Although ENN A1 and ENN B1 are structurally almost identical, dissimilarities in their chemical structure seem to lead to a different mechanism of action, a fact that has not been described to date.

Since food and feed samples commonly contain more than one

mycotoxin, as indicated by European multi-mycotoxin contamination studies (Streit et al., 2012), cytotoxic effects of binary combinations of the four ENNs were tested. In order to determine whether the co-ocurrence of toxins could enhance their toxicity, an approximation was made by combining them at 1:1 ratio. All the binary combinations tested resulted in an antagonistic effect, with the exception of ENN B1 and ENN A mixture, which presented an additive effect. This combination has been previously reported to produce additive effects in CHO–K1 and Caco-2 cells (EFSA, 2014). Therefore, co-occurrence of ENN B1 and ENN A could suppose a potential health hazard.

In conclusion, ENNs A1 and B1 alter calcium homeostasis leading to apoptotic cell death of SH-SY5Y human neuroblastoma cells. Although both ENNs present similar IC_{50} values, their mechanism of action differs since ENN A1 produced greater effects on calcium fluxes and increases ROS release. Therefore, the structural differences between ENN A1 and ENN B1 lead to dissimilarities in their mechanism of action that should be further investigated. These mechanisms of action could point to an anticancer effect of ENNs A1 and B1, however their effect in non-tumoral neurons should be assessed.

CRediT authorship contribution statement

Nadia Pérez-Fuentes: Investigation, Writing – original draft, Writing – review & editing. **Rebeca Alvariño:** Conceptualization, Methodology, Writing – review & editing. **Amparo Alfonso:** Conceptualization, Methodology, Writing – review & editing. **Jesús González-Jartín:** Investigation. **Sandra Gegunde:** Investigation. **Mercedes R. Vieytes:** Methodology. **Luis M. Botana:** Funding acquisition, Supervision.

Declaration of competing interest

The authors declare that they have no known competing financial interests or personal relationships that could have appeared to influence the work reported in this paper.

Data availability

Data will be made available on request.

Acknowledgments

The research leading to these results has received funding from the following FEDER cofunded-grants. From Conselleria de Cultura, Educacion e Ordenación Universitaria, Xunta de Galicia, GRC (ED431C 2021/01). From Ministerio de Ciencia e Innovación IISCIII/PI19/001248 and PID 2020-11262RB-C21. From European Union Interreg Agritox EAPA-998-2018, and H2020 778069-EMERTOX. R. Alvariño is supported by a postdoctoral fellowship from Xunta de Galicia (ED481B-2021-038), Spain. N.P–F. is supported by a fellowship from FIDIS, Spain.

Appendix A. Supplementary data

Supplementary data to this article can be found online at https://doi.org/10.1016/j.fct.2022.113361.

References

Alonso-Garrido, M., Frangiamone, M., Font, G., Cimbalo, A., Manyes, L., 2021. In vitro blood brain barrier exposure to mycotoxins and carotenoids pumpkin extract alters mitochondrial gene expression and oxidative stress. Food Chem. Toxicol. 153, 112261.

Alonso-Garrido, M., Tedeschi, P., Maietti, A., Font, G., Marchetti, N., Manyes, L., 2020. Mitochondrial transcriptional study of the effect of aflatoxins, enniatins and carotenoids in vitro in a blood brain barrier model. Food Chem. Toxicol. 137, 111077.

Alvariño, R., Alonso, E., Tabudravu, J.N., Pérez-Fuentes, N., Alfonso, A., Botana, L.M., 2021. Tavarua deoxyriboside A and jasplakinolide as potential neuroprotective agents: effects on cellular models of oxidative stress and neuroinflammation. ACS Chem. Neurosci. 12, 150–162.

Bertero, A., Fossati, P., Tedesco, D.E.A., Caloni, F., 2020. Beauvericin and enniatins: in vitro intestinal effects. Toxins 12.

Carreras-Sureda, A., Pihán, P., Hetz, C., 2018. Calcium signaling at the endoplasmic reticulum: fine-tuning stress responses. Cell Calcium 70, 24–31.

Chen, B.F., Tsai, M.C., Jow, G.M., 2006. Induction of calcium influx from extracellular fluid by beauvericin in human leukemia cells. Biochem. Biophys. Res. Commun. 340, 134–139.

Chou, T.-C., Talalay, P., 1983. Analysis of combined drug effects: a new look at a very old problem. Trends Pharmacol. Sci. 4, 450–454.

EFSA, 2014. Scientific Opinion on the risks to human and animal health related to the presence of beauvericin and enniatins in food and feed. EFSA J. 12, 3802.

Fotakis, G., Timbrell, J.A., 2006. In vitro cytotoxicity assays: comparison of LDH, neutral red, MTT and protein assay in hepatoma cell lines following exposure to cadmium chloride. Toxicol. Lett. 160, 171–177.

Gautier, C., Pinson-Gadais, L., Richard-Forget, F., 2020. Fusarium mycotoxins enniatins: an updated review of their occurrence, the producing Fusarium species, and the abiotic determinants of their accumulation in crop harvests. J. Agric. Food Chem. 68, 4788–4798.

González-Jartín, J.M., Rodríguez-Cañás, I., Alfonso, A., Sainz, M.J., Vieytes, M.R., Gomes, A., Ramos, I., Botana, L.M., 2021. Multianalyte method for the determination of regulated, emerging and modified mycotoxins in milk: QuEChERS extraction followed by UHPLC-MS/MS analysis. Food Chem. 356, 129647.

Huang, C.H., Wang, F.T., Chan, W.H., 2019. Enniatin B1 exerts embryotoxic effects on mouse blastocysts and induces oxidative stress and immunotoxicity during embryo development. Environ. Toxicol. 34, 48–59.

Ivanov, V.T., Evstratov, A.V., Sumskaya, L.V., Melnik, E.I., Chumburidze, T.S., Portnova, S.L., Balashova, T.A., Ovchinnikov, Y.A., 1973. Sandwich complexes as a functional form of the enniatin ionophores. FEBS Lett. 36, 65–71.

Jow, G.M., Chou, C.J., Chen, B.F., Tsai, J.H., 2004. Beauvericin induces cytotoxic effects in human acute lymphoblastic leukemia cells through cytochrome c release, caspase 3 activation: the causative role of calcium. Cancer Lett. 216, 165–173.

Kamyar, M., Rawnduzi, P., Studenik, C.R., Kouri, K., Lemmens-Gruber, R., 2004. Investigation of the electrophysiological properties of enniatins. Arch. Biochem. Biophys. 429, 215–223.

Kumar, P., Nagarajan, A., Uchil, P.D., 2018. Analysis of cell viability by the MTT assay. Cold Spring Harb. Protoc. 2018, 6, 6.

Lu, C.L., Lin, H.I., Chen, B.F., Jow, G.M., 2016. Beauvericin-induced cell apoptosis through the mitogen-activated protein kinase pathway in human nonsmall cell lung cancer A549 cells. J. Toxicol. Sci. 41, 429–437.

Manyes, L., Escrivá, L., Ruiz, M.J., Juan-García, A., 2018. Beauvericin and enniatin B effects on a human lymphoblastoid Jurkat T-cell model. Food Chem. Toxicol. 115, 127–135.

Meca, G., Font, G., Ruiz, M.J., 2011. Comparative cytotoxicity study of enniatins A, A_1, A_2, B, B_1, B_4 and J_3 on Caco-2 cells, Hep-G_2 and HT-29. Food Chem. Toxicol. 49, 2464–2469.

Meca, G., Ruiz, M.J., Soriano, J.M., Ritieni, A., Moretti, A., Font, G., Mañes, J., 2010. Isolation and purification of enniatins A, A(1), B, B(1), produced by Fusarium tricinctum in solid culture, and cytotoxicity effects on Caco-2 cells. Toxicon 56, 418–424.

Oliveira, C.A.F., Ivanova, L., Solhaug, A., Fæste, C.K., 2020. Enniatin B(1)-induced lysosomal membrane permeabilization in mouse embryonic fibroblasts. Mycotoxin Res. 36, 23–30.

Prosperini, A., Font, G., Ruiz, M.J., 2014. Interaction effects of Fusarium enniatins (A, A1, B and B1) combinations on in vitro cytotoxicity of Caco-2 cells. Toxicol. Vitro 28, 88–94.

Prosperini, A., Juan-García, A., Font, G., Ruiz, M.J., 2013. Reactive oxygen species involvement in apoptosis and mitochondrial damage in Caco-2 cells induced by enniatins A, A_1, B and B_1. Toxicol. Lett. 222, 36–44.

Prusova, N., Dzuman, Z., Jelinek, L., Karabin, M., Hajslova, J., Rychlik, M., Stranska, M., 2022. Free and conjugated Alternaria and Fusarium mycotoxins during Pilsner malt production and double-mash brewing. Food Chem. 369, 130926.

Pérez-Fuentes, N., Alvariño, R., Alfonso, A., González-Jartín, J., Gegunde, S., Vieytes, M. R., Botana, L.M., 2021. Single and combined effects of regulated and emerging mycotoxins on viability and mitochondrial function of SH-SY5Y cells. Food Chem. Toxicol. 154, 112308.

Reinholds, I., Jansons, M., Fedorenko, D., Pugajeva, I., Zute, S., Bartkiene, E., Bartkevics, V., 2021. Mycotoxins in cereals and pulses harvested in Latvia by nanoLC-Orbitrap MS. Food Addit. Contam. Part B Surveill 14, 115–123.

Rodríguez-Carrasco, Y., Narváez, A., Izzo, L., Gaspari, A., Graziani, G., Ritieni, A., 2020. Biomonitoring of enniatin B1 and its phase I metabolites in human urine: first large-scale study. Toxins 12.

Sainz, M.J., González-Jartín, J.M., Aguín, O., Mansilla, J.P., Botana, L.M., 2018. 8. Isolation, Characterization, and Identification of Mycotoxin-Producing Fungi. De Gruyter, Berlin, Boston, pp. 202–245.

Streit, E., Schatzmayr, G., Tassis, P., Tzika, E., Marin, D., Taranu, I., Tabuc, C., Nicolau, A., Aprodu, I., Puel, O., Oswald, I.P., 2012. Current situation of mycotoxin contamination and co-occurrence in animal feed–focus on Europe. Toxins 4, 788–809.

Sánchez, J.A., Alfonso, A., Leirós, M., Alonso, E., Rateb, M.E., Jaspars, M., Houssen, W.E., Ebel, R., Botana, L.M., 2015. Spongionella secondary metabolites regulate store operated calcium entry modulating mitochondrial functioning in SH-SY5Y neuroblastoma cells. Cell. Physiol. Biochem. 37, 779–792.

Tarafdar, A., Pula, G., 2018. The role of NADPH oxidases and oxidative stress in neurodegenerative disorders. Int. J. Mol. Sci. 19.

Tonshin, A.A., Teplova, V.V., Andersson, M.A., Salkinoja-Salonen, M.S., 2010. The Fusarium mycotoxins enniatins and beauvericin cause mitochondrial dysfunction by affecting the mitochondrial volume regulation, oxidative phosphorylation and ion homeostasis. Toxicology 276, 49–57.

Wätjen, W., Debbab, A., Hohlfeld, A., Chovolou, Y., Kampkötter, A., Edrada, R.A., Ebel, R., Hakiki, A., Mosaddak, M., Totzke, F., Kubbutat, M.H., Proksch, P., 2009. Enniatins A1, B and B1 from an endophytic strain of Fusarium tricinctum induce apoptotic cell death in H4IIE hepatoma cells accompanied by inhibition of ERK phosphorylation. Mol. Nutr. Food Res. 53, 431–440.

Yin, F., Boveris, A., Cadenas, E., 2014. Mitochondrial energy metabolism and redox signaling in brain aging and neurodegeneration. Antioxidants Redox Signal. 20, 353–371.